Uncertainty Analysis on CTEQ 6.1 pdf-sets using Direct Photon Production at ATLAS, LHC

Øystein Alvestad

September 30, 2008

Abstract

In this report I present the results found in an uncertainty analysis done on the CTEQ6.1 pdf-sets using direct photon production at the ATLAS experiment. The goal of the analysis is to determine how accurate the measurements of the direct photon distributions at ATLAS would have to be to contribute to improvement of the pdfs. The results showed that we might be able to contribute something to the gluon pdf using the eta distribution, but probably not the pt distribution.

Acknowledgments

First I would like to express my gratitude to Allan Clark who gave me the opportunity to work with the University of Geneva's ATLAS group this summer. To get work experience in the field of particle physics at CERN so close to the start-up of the LHC has truly been an exciting experience.

Thanks also to my excellent supervisor Andrew Hamilton for giving me a broad project to work on and for guiding me through my everyday work. Thanks for being generous with your time when I reached a dead end or needed help with the report.

Contents

Chapter 1

Introduction

In this report I present the work I did as a summer student of the University of Geneva working at the ATLAS experiment. First I wish to show how the parton density function naturally came into particle physics as a discription of composite particles. Further I briefly explain how the pdf's uncertainty can be found through the Hessian-method. The direct photon production, which is the underlying physical process this report is based on, is then explained in some detail. I also argue that the LHC collider will provide a better approach for measuring some features of the pdf than the previous high energy hadron collider, the Tevatron. This is to be reconned as the biggest motivation for undergoing this analysis. I present the methods used to obtain the simulated data used in the analysis, of course chosen to match the LHC energies and the ATLAS detector. At last I look at the results from my analysis and show that there is reason to believe that the ATLAS experiment will be able to provide data that will better define the parameter linked to the gluon distribution of the proton.

Chapter 2

Theory

In this chapter I will retrace the important steps in deriving the parton distribution function (pdf) starting from the point where one makes the proton structure approximation. The pdf is an essential part in the description of protons and its accuracy is of great importance for high energy physics (HEP) experiments like ATLAS.

2.1 From point particle to the parton distribution function

The proton is not one of the *fundamental (elementary)* particles, it is a *composite* particle. A composite particle is build up of other fundamental particles and in the protons case these are the *quarks* and the *gluons*. The quarks and gluons that build up all hadrons, like protons, are commonly known as *partons*. The structure of the proton is therefore a description of how these partons form the proton.

At the classical level and at the quantum mechanical level the importance of the proton's structure disappears, this has only relevance in the HEP regime. The reason for that is the point particle description which is assumed by todays theories at all energy- and length scale levels. At low energies the proton can be treated like a point particle whether it is a classical or quantum mechanical description, but high energies experiments show that this assumption no longer holds. Quantum field theory (QFT) is used to describe the SM and involves particles as localized fields, so all interactions described by this theory involves only point particles. Since this assumption no longer holds the proton can not be described as a QFT point particle description alone. As we will see in the next section one still exhausts as much of the succesful QFT as possible while introducing new concepts used to describe the protons substructure.

In research protons are used because they are easy to produce and accelerate in synchrotrons to the high energies required today (in contrast to electrons and neutrons). The fact that the protons underlying partons have momentum distributions is used to scan over ranges over energies which is preferable in the search for new physics.

In the late 1960s, experiments in which high energy electrons were inelastically scattered off protons were carried out at the Stanford Linear Accelerator

(SLAC). Since the early 1950s, it had been known that protons had an internal structure. By 1968 electrons were being accelerated at SLAC to 20GeV, at which energy their wavelength was such that they could resolve entities appreciably smaller than the size of the proton. [6]

The time-honored experimental method of probing structures is scattering experiments and as the citation above shows the internal structure of the proton was no exception. The scattering of an electron on a proton has different effects at different energy levels (as explained in the enumerated list below) and we need to have a look at which point in the cross section calculation we start treating the proton as a non-point like particle. Lets now see how electron proton scattering changes as we go from low center energies to energies well above 1 GeV:

1. The classical treatment of an electron proton scattering is of course the elastic process where the electron and proton emerge intact, and is considered valid for incoming electron energies $< 2.6keV$ in the laboratory frame. Electron proton scattering is the same as Rutherford scattering if you exchange the α-particle with an electron, but note that there are two major changes made in this substitution; the charge and the mass. The small mass of the electron makes it so that it has to be treated relativistically at kinetic energies above $2.6keV$ which clearly limits the classical theory. The next points will therefore treat the interaction both relativistically and quantum mechanically, and we will see how the proton should be regarded with respect to the CM energy or the energy of the incoming electron in the proton rest frame.

2. Mott scattering assumes that the proton is a point particle which does not recoil. This is a good approximation for energies $\ll M_{proton}$ (938 MeV) in the proton rest frame. The proton is three orders of magnitude heavier so the kinematic assumption can be justified at low energies. The point particle assumption sets the upper limit. A rule of thumb is that in a collision where the transferred momentum $(-q^2)$ is of the order 1 GeV a length scale of one fermi (10^{-15} m) can be probed, which is the size of the proton. So at 1 GeV the electron starts to resolve the protons inner structure and it do no longer see the proton as a point particle and the approximation becomes unsatisfactory.

3. For energies above 1 GeV we therefore have to make some assumption of the proton structure. The leading order (LO) diagram describing an electron proton scattering has an EM electron-photon vertex and a EM photon-proton vertex. The former vertex is described by quantum electrodynamics (QED) and is very well understood, while the latter vertex has its problems; the photon interacts with just one of the protons charged partons (at LO), a quark, but this quark is confined within its colour singlet and can not be treated as a free particle in the same sense that the electron does. In fact, since it is present in a field of the strong force, the quark interacting at the proton vertex is very likely to be virtual. Since we measure the outgoing electrons energy and angular distribution the first change in the standard QED calculation is made in the following differential cross section: $\frac{d\sigma}{dE'd\Omega} = \frac{\alpha^2}{q^4}\frac{E'}{E}(L^e)^{\mu\nu}W_{\mu\nu}$. $(L^e)^{\mu\nu}$ is the lepton tensor describing the electron-photon vertex, while the $W_{\mu\nu}$, the proton tensor,

is an approximation describing the photon-proton vertex. E and E' is the incoming and outgoing energy of the electron respectively. The tensor product $(L^e)^{\mu\nu} W_{\mu\nu}$ is an attempt to parametrize the invariant amplitude $\langle |M|^2 \rangle$.

The $W_{\mu\nu}$ is constructed in its most general physical form out of two kinematically independent fourvectors at the photon-proton vertex, p_2^μ and q^μ (see figure 2.1). In its reduced form $W_{\mu\nu}$ has terms linear in $W_{1,2}$ which are functions of either q^2 in the elastic case or q^2 and $x = \frac{-p*q}{q^2}$ in the inelastic case. The inelastic tensor reduces to the elastic one if one puts the elastic constraint on the outgoing momentum of p_4 that $p_4^2 = p_2^2 = M_{proton}^2$, that is the invariant mass of the proton (and the proton itself of cours) is preserved through the interaction.

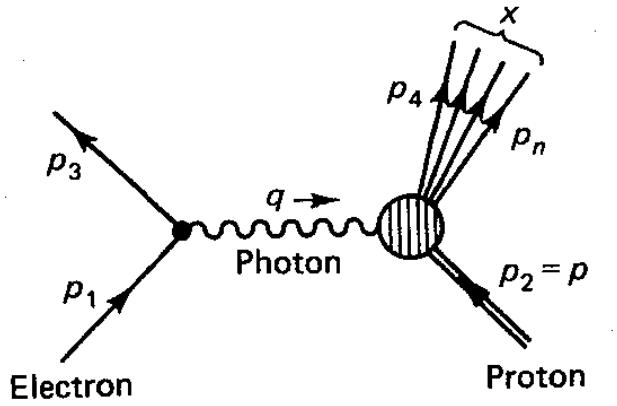

Figure 2.1: Inelastic electron-proton scattering [4]

The electrons that transfer their full momenta no longer scatter of the point particle proton but the protons charged point particle constituents. Experimentally one also observes that inelastic scatterings start to appear; after the collision the electron emerges together with hadronic debris coming from the photon-proton vertex. This happens because the scattered quarks momentum is so large that it is able to stretch the proton into a length scale where the strong field becomes very high. This potential energy is formed into matter when two quarks is pair created out of the vacuum in this field, so that we now have two hadrons. This was a crude explanation of what is known as fragmentation, but the over all effect is that some of the scattered quarks momentum is transferred into mass which comes out of the process.

4. Above an energy threshold of tens of GeV the time dilatation becomes so strong that at interaction time the quark that is scattered can be treated as a free particle again. The three quarks inside the proton interact with each other and the vacuum all the time, but in what is known as the deep

inelastic scattering (DIS) regime these processes occur on a longer time scale than the EM interaction with the electron. At these energies $-q^2$ is likely to be above the limit (1 (GeV)^2) where $W_{1,2}$ becomes functions of only x, which can be interpreted as the quarks momentum fraction of the proton's. Since the quarks are relatively free to move inside the proton one would assume that this fraction would not be the same each time but have some probability distribution $f(x)$, also known as a quark distribution function (qdf). The qdf is part of a what we call pdfs which treats both quarks and gluons.

We have seen in this section how it is the quarks inside the proton which undergoes an interaction in the DIS and that they can be treated as free particles at sufficiently high energies. In hadron hadron colliders like the LHC both of the two parton types will take part in the initial interactions as they are mainly governed by the strong force. Infact, at the LHC, the gluons are actually the most likely parton to make hard collisions as they are more likely to carry a considerable amount of the proton's momentum. This is predicted by the pdf which we in the following section will take a closer look at.

2.2 More on pdfs

Inside a hadron one usually divides the particles into three groups; *the valence quarks* which are always present and constitute the colour singlet, *the gluons* which mediate the strong colour field which confines the valence quarks and at last *the sea quarks* which are the quark anti-quark pairs created in loops made by the virtual gluons. As we shall see below there exists different pdfs at different $-q^2$, and the differences are of great importance; i.e. at high $-q^2$ the sea quarks play an important role since the timescale of the interaction is short compared to the time between creation and annihilation of the pair inside the loop, while at low $-q^2$ the seaquark contribution is therefore less substantial. Figure 2.2 shows a NLO pdfs representing particles from all of the three major groups. See for instance how the seaquark ($\bar{u}$) is compareable to the valence quark (u) in the low x-region, while it is much less likely to carry a large fraction of the hadrons momentum.

A definition of the pdf is: *The parton distribution functions give, at some order of magnitude, the probability density for finding a particle with a certain longitudinal momentum fraction x at momentum transfer $-q^2$.* Pdfs were first introduced in the DIS, as explained above, but Drell and Yan proposed over 30 years ago that the DIS-formalism could be extended to pure hadron hadron collisions. The trick was to identify the LO subprocess (e.g. $q\bar{q} \to l^+l^-$ is the LO subprocess in a Drell Yan process) and calculate its invariant cross section. Then they weighted the cross section with pdfs and integrated over the quarks momentum: $\sigma_{AB} = \int dx_a dx_b f_{a/A}(x_a) f_{b/B}(x_b) \hat{\sigma}_{ab\to X}$. The model had great success (not only for the Drell Yan process). When calculating NLO perturbative corrections divergences due to collinear gluon emission made the cross section expansion diverge. The divergence came from the familiar logarithmic terms seen in all hard-scattering processes and could be treated by letting the pdfs absorb the logarithmic terms (via the DGLAP equations) and then let the pdfs be renormalized. The pdfs then became functions of a second variable

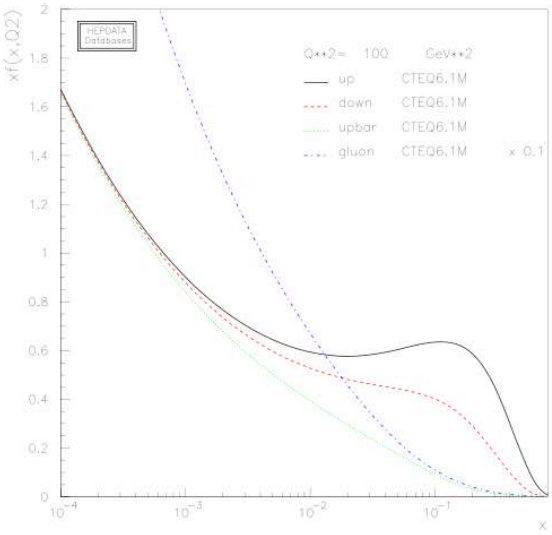

Figure 2.2: The CTEQ6.1 parton distribution function evaluated at a Q of 10GeV [1]

namely a large momentum scale factor ($\mu_f^2 = -q^2$). With this correction another problem occured; the finite cross sections were no longer universal. This was solved by introducing a cross section perturbation series in the running coupling constant $\alpha_s(\mu_r^2)$ (where μ_r^2 is the renormalization scale). The two scaling parameters are usually set equal to the same suitable momentum scale constant of the hard scattering process, and the pdfs dependency on μ_f^2 is calculated from the DGLAP equations. The x-dependency is however best described when fitted from various data samples, in example DIS experiments.

At new experiments which probe at increasing energies there are no data available for the pdf-fits. As we have already seen the pdfs are essential in calculating the cross sections for interesting physics and their backgrounds, so to be able to make some predictions we need a new pdf at our energy scale. In these cases one calculate the cross sections of the processes which contribute with data to a preferred order in α_s and make a global fit with existing data. With the global fit one can get a pdf at any given $-q^2$, which was exactly what we needed. The data used in the global fit comes mainly from three different types of experiments; DIS, Drell Yan and jet production (from the DIS and the Drell Yan the data is extracted from measuring the hadron structure functions which was discussed above). Recently many cross sections have been calculated to next to next to leading order (NNLO), but these does not include jet production processes. Therefore NNLO global fits are still approximate, while the NLO and LO are both fully calculated to their order of magnitude. In contradiction to pdf analyzists recomendations some experiments still use the LO pdfs instead of the NLO since they would like to match the order of magnitude of the Monte Carlo (MC) generators, which still usually run at LO. The difference between the LO and NLO pdfs are considerable; for many important pdfs the LO pdf lies outside the 1-σ errorband of the NLO pdf. (There would still be a caveat if one used a NLO pdf in physics analysis, the real test would be done with a NLO MC).

In the CTEQ global fitting procedure there is a number of free parameters

(20 in our study) which are tuned in the fit. These parameters have uncertainties connected to the data sets they were taken from and their appearance in the fit. To make a complete analysis the variation in the cross sections due to the pdfs should be calculated, and one of the popular precedures is the Hessian technique. One starts by diagonalizing the Hessian matrix which has a dimension equal to the number of free parameters. This leaves you with the same number of eigenvectors which are now, in general, functions of all the free parameters. By stepping a number of σ's in either eigenvector-direction you find the uncertainty on that eigenvalue. Sometimes there is a high correlation between one parameter and an eigenvector and the pdf dependency on that variable is seen trivially from varying around one eigenvalue. The maximal uncertainty for one of the free parameters can although still be retrieved by defining a master equation where one takes the square-root of the sum of maximal difference in each +/- eigenvector-direction in quadrature.

2.3 Direct photon production

A direct photon (DP) is a photon produced in the primary parton-parton interaction. The DP distribution is valuable to both experimentalists and theorists. At the LO the final state particles in DP production are a photon and either a quark or a gluon. Since in a back to back scattering (in the Φ-plane) the final state particles' energies are related, we can use the superior energy resolution of the electromagnetical calorimeter, measuring the photon, to calibrate the hadronic calorimeter, measuring the jet from the final state quark or gluon. Cross section measurements of DP processes will give us valuable information about perturbative QCD, again due to the simplicity of the photon detection together with the EM vertex giving more reliable higher order calculations. At last the DP distribution gives good data in determining the gluon contents in the pdfs, which will be discussed in further detail below.

As seen in the four Feynman diagrams, shown in figure 2.3 and 2.4 below, DP are produced from either an annihilation process or a Compton scatter process, at LO. Which one of these two processes is dominant in an experiment is determined by which particles are collided and on the choice of interval you make for the kinematic variables in your study. At Tevatron, where they collide protons with anti-protons the annihilation process is far more likely than at the LHC, a proton proton collider, where the Compton scatter contribute 80-90%. Therefore the LHC will produce superior statistics on the Compton cross section in comparison to Tevatron not only bacause of the technical improvements of the collider, but because the pdf of one of the collided particles is different in the two experiments. The Compton scatter DP cross section is clearly dependent on the gluons pdf which we will see in the result section is badly understood. Therefore new data from the LHC is likely to make improvements on the pdf when the statistics become good enough. This was one of the main motivations to undergo the simulations on the pdf uncertainties presented in this report. However we shall see that there are also other eigenvalues of the diagonalized Hessian which have high uncertainties which may be improved by DP analysis.

Finally it should be noted that although DP is a nice process to study at LO, higher order processes disrupt the nice back to back feature of the process. An example is the NLO DP production when during the fragmentation process a

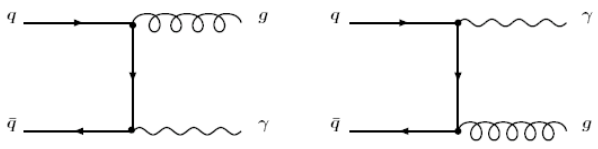

Figure 2.3: The LO Annihilation diagrams

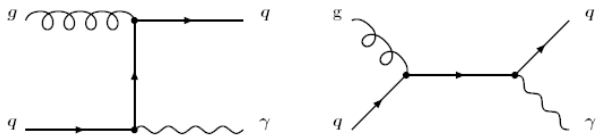

Figure 2.4: The LO Compton diagrams

bremsstrahlung photon is emmited. Especially brehmsstrahlung photons emitted at a large angle are hard to discriminate and they actually contribute at the same order of magnitude as the LO order processes (even though it is atleast a NLO process). Also relativistic $\pi^0 s$ decaying with collinear photons are hard to distinguish and is a common background process.

Chapter 3

Methods

All of the simulation work which this report is based upon was done on ATLAS' computer framework Athena. Athena is based on C++ and can be used for all offline data -processing and -analysis. The framework also offers you to run your MC and detector simulations, which was undergone in my analysis. In the analysis of the simulated data I used ROOT which is an object-oriented data analysis framework. The methods used to obtain the results presented in the next chapter can naturally be divided into three parts; Generation, Detector simulation and Analysis.

3.1 Generation

The MC used for generating events was PYTHIA version 6.412. I was interested in direct photon production at the LHC so I simulated proton proton collisions at CM energy of 14 TeV. I exclusively produced the two LO direct photon processes namely the $2 \rightarrow 2$ hard scattering processes $f + \bar{f} \rightarrow \gamma + g$ and $f + g \rightarrow f + \gamma$ along with the semihard interactions made by the spectator partons. A kinematic cut was applied to the $\hat{p}_T$ with lower bound at 45 GeV. Since I wanted to study the uncertainty of the different eigenvalues on the pdf I generated events using the 40 different, 20 parameters multiplied by the two directions (+/-) in σ, errorsets from the CTEQ6.1-series (Les Houches numbers from 10001-10040) along with the meanset and the two LO fits from CTEQ6.1 (Les Houches numbers 10000 and 10041-42 respectively) for comparison. At first I generated 10000 events for each pdf, but due to too few statistics I was forced to generate around 1 million events per pdf.

3.2 Detector simulation

The simulation of the ATLAS detector takes a lot of resources and a faster approach called Atlfast has been developed for the same purpose. Instead of simulating the detection of each generated particle you use statistics (obtained from the full analysis) to smear out the generated events. In my simulation the fast Atlfast precedure was chosen and I used standardised files for Athena version 13.0.40.1. Since all the analysis were performed on truthparticles none of the effects from the detector simulation were used, but I accessed the truthparticle

data through the same framework as one would use with the detector data. To compare observations at truthparticle level with the simulated data from the detector would be useful, so the detector data should be useful in a further analysis.

3.3 Analysis

The analysis part made histograms of the p_T distribution and the η distribution of the direct photons at truth particle level. The histograms were created as objects following the ROOT-standard.

After these initial processes all the work could be done with the help of the ROOT-framework. The results are prestented in the next chapter.

Chapter 4

Results and Discussion

Here I present the results from the uncertainty analysis on the CTEQ6.1 pdf-set at LHC CM energy of 14 TeV. All plots were obtained as explained in the Methods chapter.

4.1 η distribution

Figure 4.1 shows a typical η-distribution. Allthough the number of events simulated for pdf error-set 30 is close to 2 million this is not the case for all the pdfs, the majority of the 40 different error-set pdfs have just below one million events simulated.

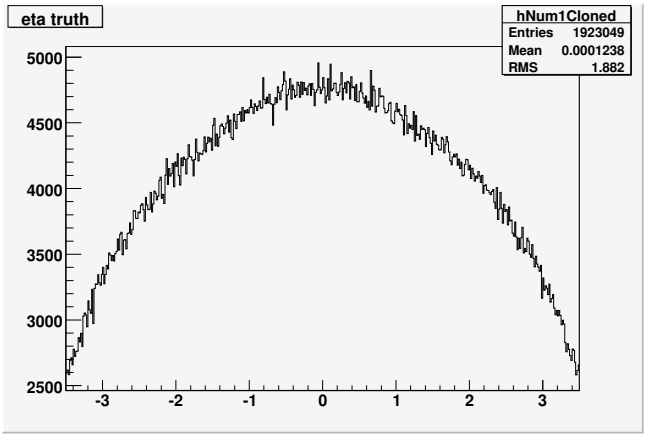

Figure 4.1: The η-distribution for error set 30

The psuedorapidity distributions are the only distributions showing large statistical fluctuations for some of the normalized Hessian-eigenvalues. In figure 4.2 below the relative difference between the η-distribution with statistics of

error-set 30 and the mean is plotted ($\frac{\eta(pdf_{errorset_{30}})-\eta(pdf_{mean})}{\eta(pdf_{mean})}$). Since the number of simulated events were different the sets I normalized each distribution before performing the task mentioned. The only feature that may display a difference from zero in these plots are the shape of the distributions.

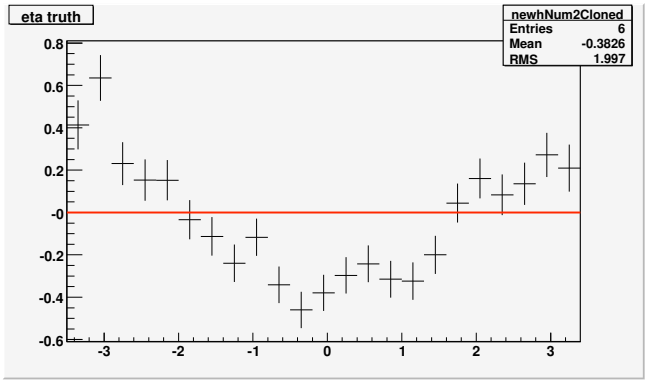

Figure 4.2: Statistics of the relative difference to the mean for η-distribution for error set 30 with 1 million events

The statistics of the relative difference plot in figure 4.2 is shown in figure 4.2. They are calculated as the square root of the number of entries per bin. As mentioned in the Methods chapter the statistics were not good enough at 10000 events and a plot of the statistics of the relative difference in for 10000 events is shown in 4.3. We also see that the distribution

The region of greatest interest is $|\eta| < 2.5$ since only in this region can the ATLAS detector provide tracks of the particles, which is vital in discriminating i.e. electrons from protons. We see that for error set 30 there is clearly room for improvement as it is up to 40% different from the mean with an uncertainty of roughly 10%. The eigenvalue 15 (corresponding to error-set 29 and 30) is one of the eigenvalues largely dependent upon one of its parameters; the gluon distribution in the proton. This distribution is clearly important in the Compton scattering process (mentioned in section 2.3) which is so dominant at the LHC. In appendix .1 you can see large figures of five other interesting histograms together with the relative difference of all 40 error-sets. The ones of interest are always plotted together with the second error-pdf belonging to the same variable. The reason for that is to look for symmetries and asymmetries, since an asymmetry generally means that there is a large uncertainty connected to that eigenvalue and symmetric eigenvalues are relativly well defined. Inclusive jet production simulations for the CTEQ6.1 error-sets at the Tevatron showed that the ten first eigenvalues (corresponding to the 20 first error-pdfs) are relatively well-defined. That we therefore find some tendencies of asymmetry in eigenvalue 10 is therefore interesting. The two eigenvalues above 10 (namely 11 and 15)

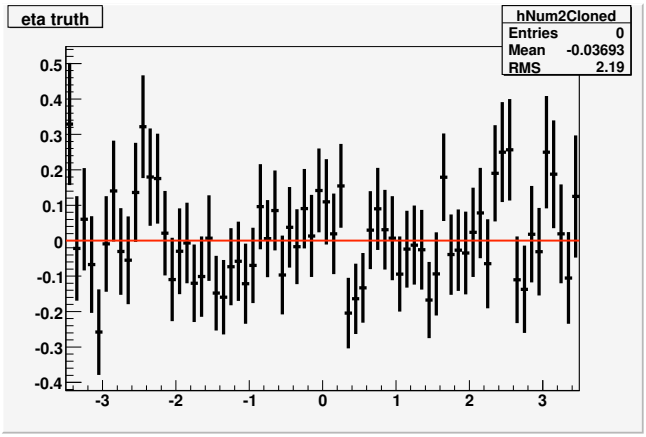

Figure 4.3: Statistics of the relative difference to the mean for η-distribution for error set 30 with 10 thousand events

show asymmetries as expected.

4.2 p_T distribution

A typical p_T-distribution is shown in figure 4.4. The number of events simulated per pdf-set is of cours the same as in the η-distributions. Further I present the relative difference to the mean of p_T-distribution with statistics for error set 6 in figure 4.5.

The region of interest for the p_T-distribution is above 50-60 GeV because of the p_t-kick problem (which seems to have been resolved at NLO [5], but ATLAS still uses LO pdfs). The upper bound in an experimental situation is dependent upon the amount of time you collect data. In my simulations it is roughly 130 GeV because the distribution falls off qiuckly and one does not have enough events to produce good statistics above this limit. A nice way of showing this upper limit is by looking at the high end of the relative difference to the mean of p_T-distribution with statistics for error set 10 shown in figure 4.6, the statistics grow large in the regions where the relative difference is the biggest, while in the η-case we had good statistics in these regions.

One dose not find a big difference in shape in the p_T-distributions of the error sets compared to the mean. All plots can be viewed in appendix .2.

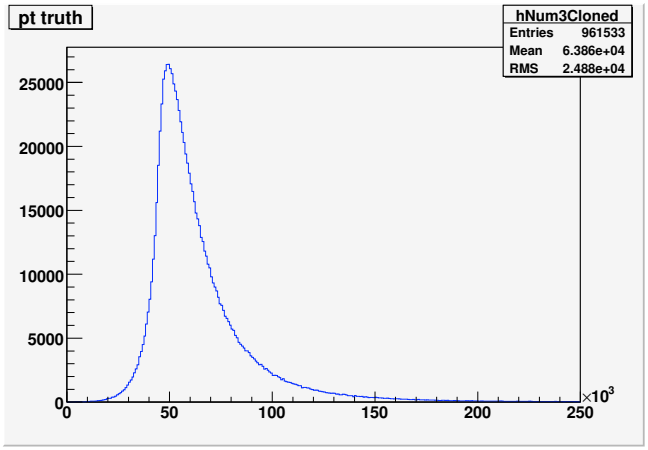

Figure 4.4: The p_T-distribution for error set 6

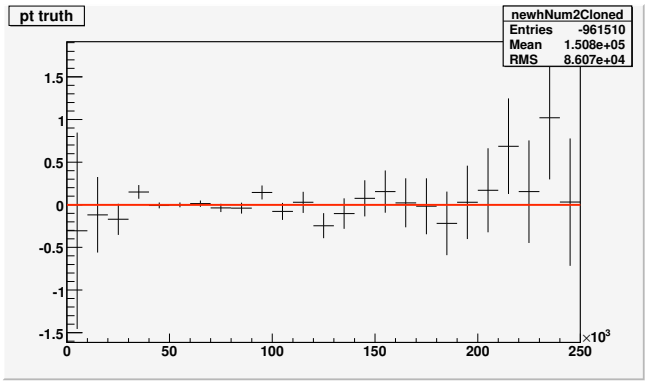

Figure 4.5: Statistics of the relative difference to the mean for p_T-distribution for error set 6 with 1 million events

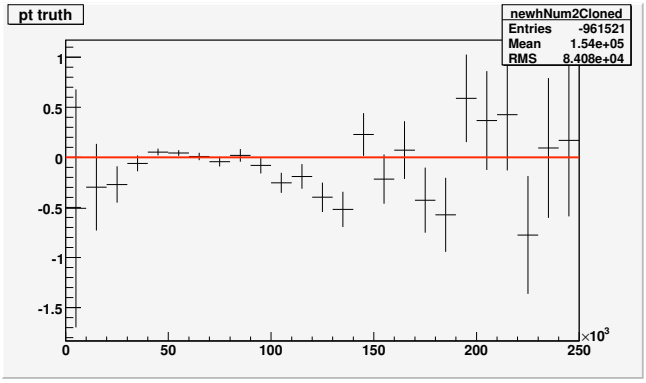

Figure 4.6: Statistics of the relative difference to the mean for p_T-distribution for error set 10 with 1 million events

Chapter 5

Appendix

.1 η distribution plots

The figures holding more than one histogram are all arranged in a specific order. The upper most to the left is the one with the lowest number and you increase this number by one for each step to the right and increase it by four for each step made downward. In figure 1 the plot of the relative difference of pdf error-set nine is therefore the one in the lower left corner.

In figure 4 it should be emphasized that pdf 41 and 42 has nothing to do with the error-sets, but are two LO pdfs (in contrast to the mean set which is NLO) with different global fits. They illustrate the huge expected difference mentioned in theory chapter.

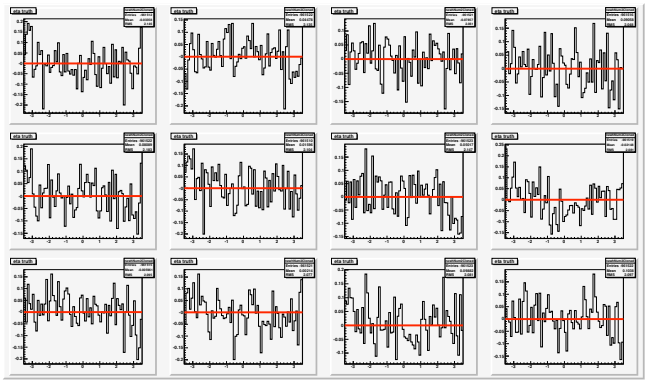

Figure 1: The relative difference to the mean of η-distribution for pdf error-set 1 to 12

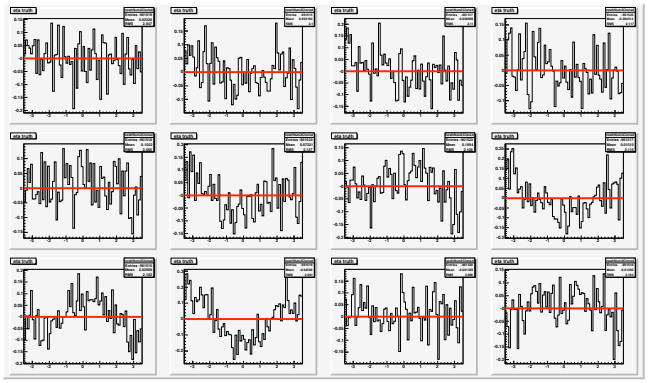

Figure 2: The relative difference to the mean of η-distribution for error set 13 to 24

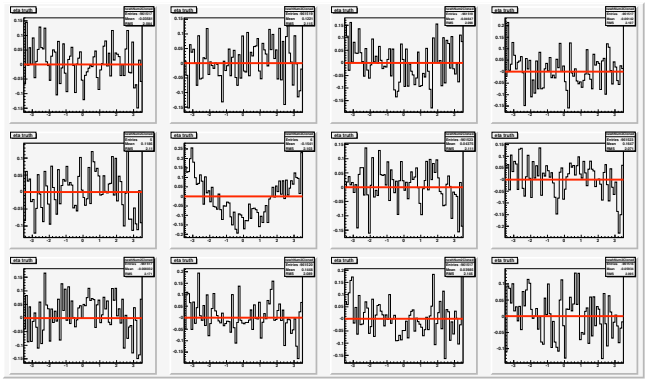

Figure 3: The relative difference to the mean of η-distribution for error set 25 to 36

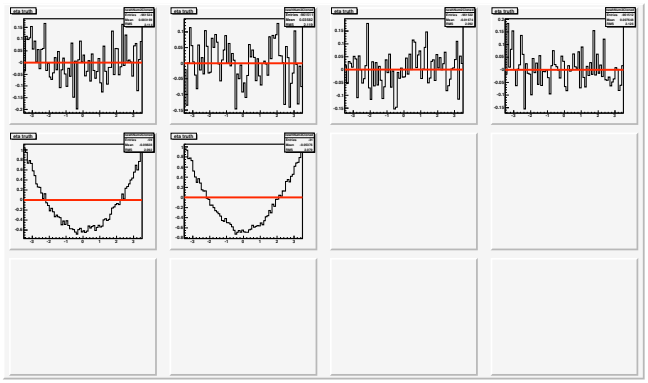

Figure 4: The relative difference to the mean of η-distribution for error set 37 to 42

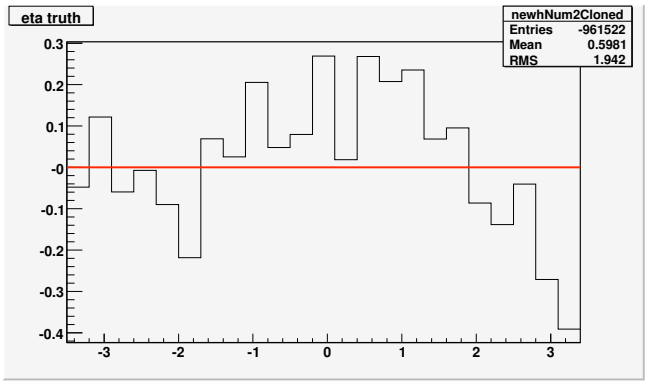

Figure 5: The relative difference to the mean of η-distribution for error set 19

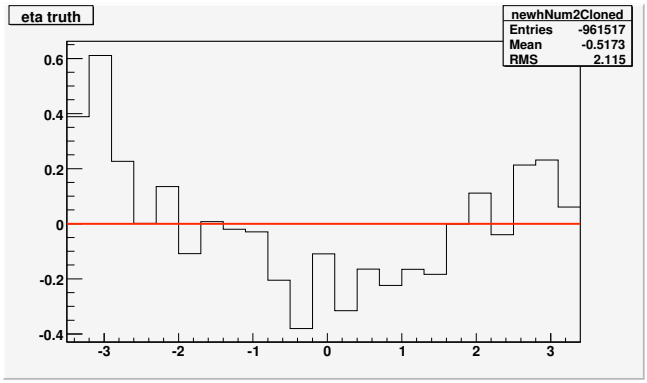

Figure 6: The relative difference to the mean of η-distribution for error set 20

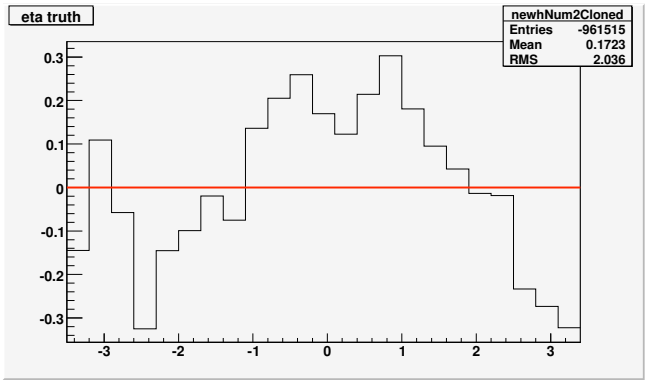

Figure 7: The relative difference to the mean of η-distribution for error set 21

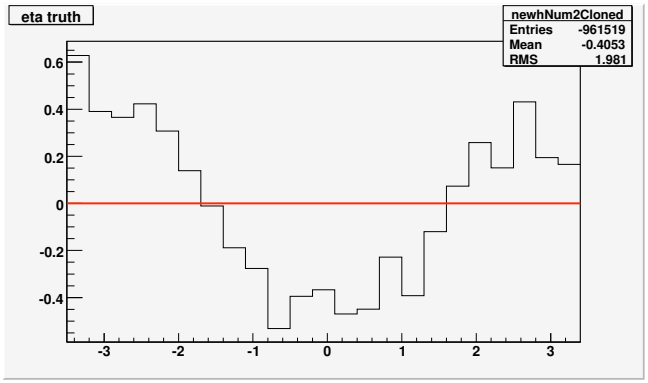

Figure 8: The relative difference to the mean of η-distribution for error set 22

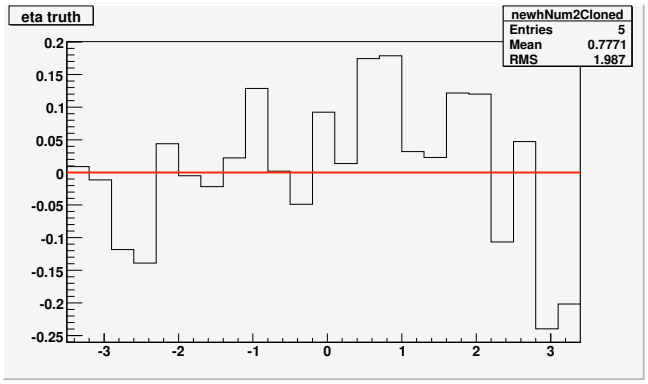

Figure 9: The relative difference to the mean of η-distribution for error set 29

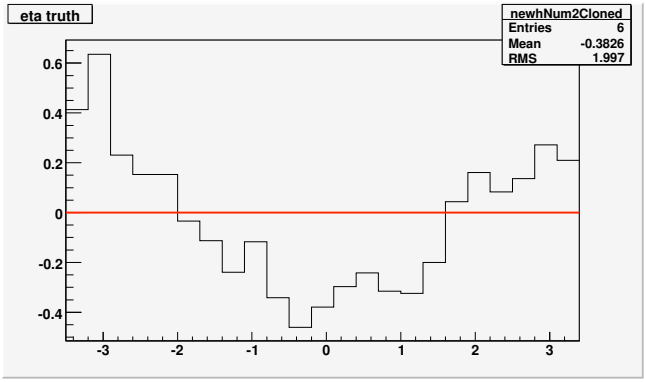

Figure 10: The relative difference to the mean of η-distribution for error set 30

.2 p_T distribution plots

The figures holding more than one histogram are all arranged in the same specific order as explained for the η-distribution part. The remarks made on pdf 41 and 42 are valid for the p_T-distribution also of cours.

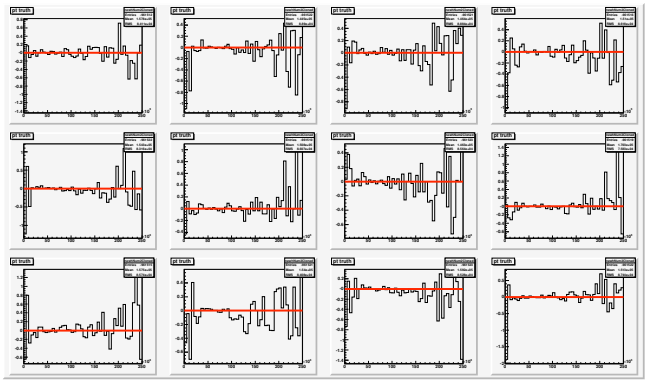

Figure 11: The relative difference to the mean of p_T-distribution for pdf error-set 1 to 12

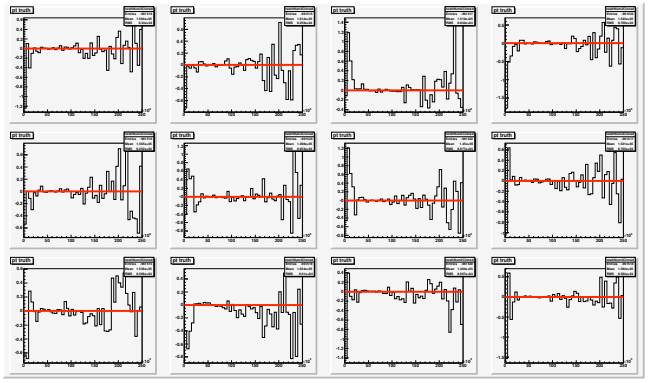

Figure 12: The relative difference to the mean of p_T-distribution for error set 13 to 24

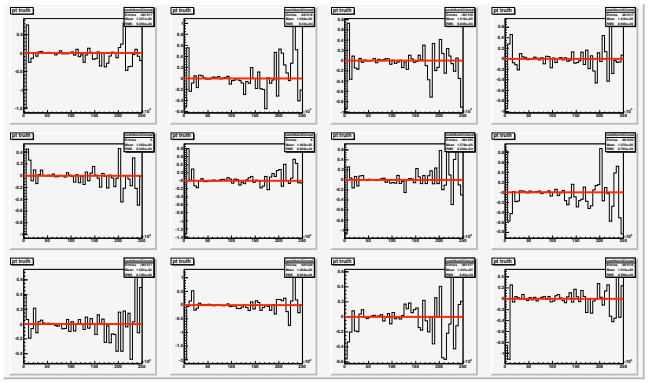

Figure 13: The relative difference to the mean of p_T-distribution for error set 25 to 36

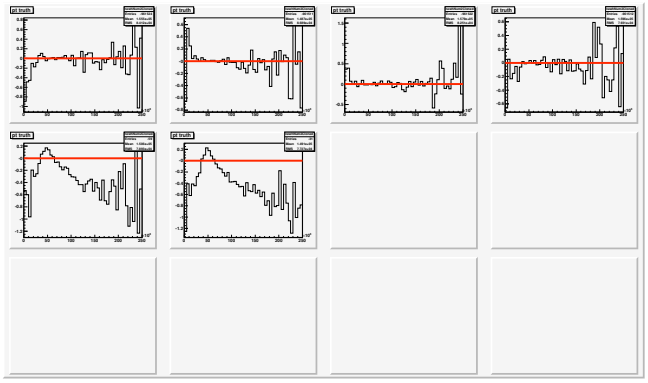

Figure 14: The relative difference to the mean of p_T-distribution for error set 37 to 42

Bibliography

[1] J M Campbell, J W Huston and W J Stirling *Hard interactions of quarks and gluons: a primer for LHC physics* 2006 stacks.iop.org/RoPP/70/89

[2] Thomas Ivan Hollins *SCT Hybrid Testing and the Production of Direct Photons in the ATLAS experiment at the LHC* CERN-THESIS-2007-061

[3] Francis Halzen, Alan D. Martin *Quarks & Leptons: An introductory course in modern particle physics* Published by WILEY-VCH, 1984 ISBN 0-471-88741-2

[4] David Griffiths *Introduction to Elementary Particles* Published by WILEY-VCH, 1987 ISBN-13 978-0-471-60386-3

[5] P. Aurenche et. al. *A new critical study of photon production in hadronic collisions* 2006 arXiv:hep-ph/0602133v2

[6] David C. Lindberg, Roy Porter, Ronald L. Numbers, Mary Jo Nye *The Cambridge History of Science* Published by Cambridge University Press, 2003 ISBN 0521571995, 9780521571999